

Surface and Interface Processes during Atomic Layer Deposition of Copper on Silicon Oxide

Min Dai,[†] Jinhee Kwon,[‡] Mathew D. Halls,[§] Roy G. Gordon,^{||} and Yves J. Chabal^{*‡}

[†]Laboratory for Surface Modification, Rutgers University, Piscataway, New Jersey 08854, [‡]Materials Science and Engineering, the University of Texas at Dallas, Richardson, Texas 75080, [§]Materials Science Division, Accelrys Inc., San Diego, California 92121, and ^{||}Department of Chemistry and Chemical Biology, Harvard University, Massachusetts 02138

Received August 27, 2009. Revised Manuscript Received December 30, 2009

The initial surface chemistry and growth mechanisms of the atomic layer deposition (ALD) of metallic copper on SiO₂ surfaces are investigated using an amidinate precursor (copper(I) di-*sec*-butylacetamidinate, [Cu(^sBu-amd)]₂) and molecular hydrogen. Using in situ Fourier transform infrared spectroscopy together with calculations based on density functional theory, we show that the initial surface reaction of [Cu(^sBu-amd)]₂ with hydroxylated SiO₂ takes place by displacement of one of the *sec*-butylacetamidinate ligands at a surface –OH site, thus forming a Si–O–Cu–(^sBu-amd) surface species, evident by the stretching vibrations of Si–O–Cu and the chelating –NCN– bonds. Molecular hydrogen exposure during a subsequent pulse dissociates most of the *sec*-butylacetamidinate ligands bound to surface Cu, which releases free amidine vapor, leaving Cu atoms free to agglomerate on the surface and thus opening more reactive sites for the next [Cu(^sBu-amd)]₂ pulse. Copper agglomeration is evident in the IR absorbance spectra through the partial recovery of the intensity of SiO₂ optical phonon modes upon H₂ reduction, which was lost after the reaction of [Cu(^sBu-amd)]₂ with the initial SiO₂ surface. The thermally activated ligand rearrangement from a bridging to a monodentate structure occurs above 220 °C through hydrogenation of the ligand by surface hydroxyl groups after exposure to a [Cu(^sBu-amd)]₂ pulse. As Cu particles grow with further ALD cycles, the activation temperature is lowered to 185 °C, and hydrogenation of the ligand takes place after H₂ pulses, catalyzed by Cu particles on the surface. The surface ligand rearranged into a monodentate structure can be removed during subsequent Cu precursor or H₂ pulses. Finally, we postulate that the attachment of dissociated ligands to the SiO₂ surface during the [Cu(^sBu-amd)]₂ pulse can be responsible for carbon contamination at the surface during the initial cycles of growth, where the SiO₂ surface is not yet completely covered by copper metal.

Introduction

Atomic layer deposition (ALD) is one of the most attractive methods to grow uniform, conformal thin films with a high degree of control over film thickness and composition due to its self-limiting surface reactions. ALD has been successfully developed to grow many metal oxides.¹ Interest in Cu metallization is increasing as a result of a variety of industrial applications, including the needs of microelectronics for 22 nm transistors. Copper is replacing aluminum as an interconnect material in integrated circuits because of its lower resistivity ($1.72 \times 10^{-6} \Omega \cdot \text{cm}$ vs $2.82 \times 10^{-6} \Omega \cdot \text{cm}$) and higher stability against electromigration. For these applications, a highly conformal and continuous copper seed layer is required before subsequent electrochemical deposition of a copper film with a high growth rate. The growth of transition metal films by ALD, however, has shown limited success.^{2,3} One of the reasons for these difficulties is a lack of suitable precursors that satisfy the stringent requirements of ALD, such as thermal stability, high volatility, and efficient self-limited reactivity with surfaces.⁴ Another reason is the poor understanding of the growth mechanisms for metal ALD, particularly when compared to that for ALD-grown metal oxides.

Several aspects of the growth of Cu films using ALD have been addressed. A few copper(I) and copper(II) precursors have been used in the past, such as CuCl,^{3,5} Cu(II)-2,2,6,6-tetramethyl-3,5-heptandionate [Cu(thd)]₂,^{6,7} Cu(II)-1,1,1,5,5,5-hexafluoro-2,4-pentanedionate [Cu(hfac)]₂,^{8,9} and Cu(II) acetylacetonate [Cu(acac)]₂,^{10,11} but all suffer from undesirable properties as ALD precursors.¹² For example, CuCl has very low vapor pressure, and Cu films deposited by Cu(hfac)₂ contain fluorine, which hinders Cu adhesion on the substrate. They all have very low reactivity and low growth rate. Therefore, higher deposition temperatures are required (> 200 °C), which fosters unwanted Cu agglomeration and diffusion.^{12–14} In other cases, the lack of self-limiting surface chemistry for ALD of Cu resulted in coarse polycrystalline grains of as-deposited films.^{15,16} In general, a systematic study

*To whom correspondence should be addressed. E-mail: chabal@utdallas.edu.

(1) Suntola, T. *Atomic Layer Epitaxy*; Blackie Academic and Professional: London, 1990.

(2) Lim, B. S.; Rahtu, A.; Gordon, R. G. *Nat. Mater.* **2003**, *2*, 749–754.

(3) Marika, J.; Mikko, R.; Markku, L. *J. Vac. Sci. Technol., A* **1997**, *15*, 2330–2333.

(4) Musgrave, C.; Gordon, R. G. *Future Fab Int.* **2005**, *18*, 126–128.

(5) Martensson, P.; Carlsson, J.-O. *Chem. Vap. Deposition* **1997**, *3*, 45–50.

(6) Per, M.; Jan-Otto, C. *J. Electrochem. Soc.* **1998**, *145*, 2926–2931.

(7) Christopher, J.; Lanford, W. A.; Christopher, J. W.; Singh, J. P.; Pei, I. W.; Jay, J. S.; Toh-Ming, L. *J. Electrochem. Soc.* **2005**, *152*, C60–C64.

(8) Raj, S.; Balu, P. *Electrochem. Solid-State Lett.* **2000**, *3*, 479–480.

(9) Huo, J.; Solanki, R.; McAndrew, J. J. *Mater. Res.* **2002**, *17*, 2394–2398.

(10) Utraiainen, M.; Kröger-Laukkanen, M.; Johansson, L.-S.; Niinistö, L. *Appl. Surf. Sci.* **2000**, *157*, 151–158.

(11) Antti, N.; Antti, R.; Timo, S.; Kai, A.; Mikko, R.; Markku, L. *J. Electrochem. Soc.* **2005**, *152*, G25–G28.

(12) Li, Z.; Rahtu, A.; Gordon, R. G. *J. Electrochem. Soc.* **2006**, *153*, C787–C794.

(13) Benouattas, N.; Mosser, A.; Raiser, D.; Faerber, J.; Bouabellou, A. *Appl. Surf. Sci.* **2000**, *153*, 79–84.

(14) McBrayer, J. D.; Swanson, R. M.; Sigmon, T. W. *J. Electrochem. Soc.* **1986**, *133*, 1242–1246.

(15) Per Martensson, J.-O. C. *Chem. Vap. Deposition* **1997**, *3*, 45–50.

(16) Juppö, M.; Ritala, M.; Leskela, M. *J. Vac. Sci. Technol., A: Vac., Surf., Films* **1997**, *15*, 2330–2333.

of Cu agglomeration and diffusion as a function of substrate temperature has not been carried out. Also, the surface chemistry controlling the film purity has not been fully explored, making it difficult to assess existing and new precursors. Therefore, the lack of detailed mechanistic studies of metal ALD hinders the development of suitable precursors and its full application in industry. Furthermore, the chemistry involved in the deposition of mono-elemental metallic films by ALD is a fascinating area of research in its own right because it is intrinsically complex.

In this work, we study the initial surface chemistry and growth mechanisms of the ALD of copper on the SiO₂ surface using an amidinate precursor (copper(I) di-*sec*-butylacetamidinate, [Cu(⁸Bu-amd))₂) and molecular hydrogen (H₂). The choice of precursor is motivated by the recent report that metallic copper could be grown with high conformality and high conductivity using this precursor.¹⁷ Combining in situ Fourier transform infrared spectroscopy (FTIR) and ex situ X-ray photoelectron spectroscopy (XPS), we investigate the initial reaction pathways of ALD involving the interaction of OH-terminated SiO₂ with [Cu(⁸Bu-amd))₂ and the subsequent ligand reduction, rearrangement, and removal upon H₂ exposure. Evidence for Cu agglomeration and impurity incorporation under the growing film is presented. Density functional theory (DFT) is used to determine the vibrational signatures of the relevant chemical species involved during the deposition process in order to corroborate critical experimental band assignments.

Experiments and Results

Double-side polished, float-zone grown, and lightly doped (~10 Ω·cm) Si(100) with thin thermal oxide (6–10 nm thick SiO₂) is used as the substrate. The sample is first rinsed by acetone, methanol, and deionized water (18.2 MΩ·cm), and standard RCA¹⁸ cleaning is performed followed by thorough rinsing with deionized water and blow-drying with N₂. Then the sample is immediately loaded in the ultra pure N₂ (oxygen impurity <10^{−3} ppm) purged ALD chamber.

All experiments are done in a homemade ALD system integrated with a Thermo Nicolet 670 interferometer for in situ FTIR measurements.¹⁹ A single-pass transmission geometry is used with an incidence angle close to the Brewster angle to maximize transmission, minimize interference, and increase sensitivity to absorptions below ~1500 cm^{−1}. Normal incidence measurements are also performed to help distinguish perpendicular from parallel components (to the surface) in the infrared (IR) spectra. A 400–4000 cm^{−1} spectral range is investigated with a resolution of 4 cm^{−1}.

The precursor [Cu(⁸Bu-amd))₂] is kept at 95–100 °C, and purified N₂ is used as the carrier gas to deliver the copper precursor. Copper films are deposited by introducing [Cu(⁸Bu-amd))₂] (exposure ~10⁷ L) and H₂ (exposure ~10¹¹ L) (ultra high purity, 99.999%, purified by Aeronex Gate Keeper gas purifiers) alternatively into the ALD chamber. During deposition, the substrate temperature is kept at 185 °C for optimum Cu deposition.¹² After each precursor dose, the ALD chamber is purged with N₂ and pumped thoroughly to reduce background contamination. The substrate temperature during infrared absorbance measurements is maintained at 60 °C (i.e., slightly above room temperature) in

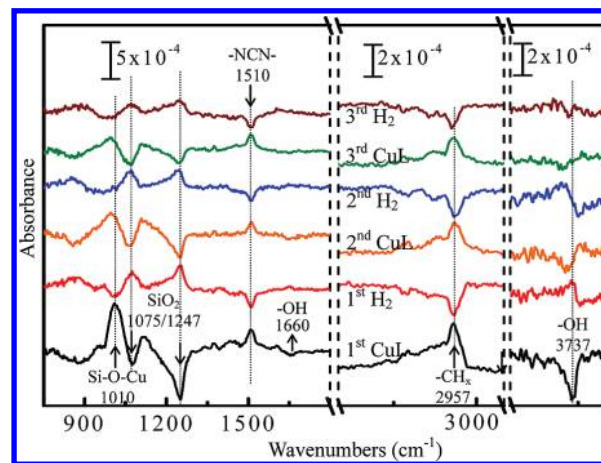


Figure 1. Differential absorbance spectra of the first three cycles of Cu ALD on SiO₂ at 185 °C. Each spectrum is referenced to that of the previous half cycle and the bottom (“1st CuL”) is referenced to the initial oxide surface. The incident angle of infrared beam is 74° (~Brewster angle).

order to have temperature control within 0.5 °C to suppress any thermal artifacts due to bulk Si phonon vibrations.

First-principles calculations based on DFT are carried out to aid in the interpretation of key infrared bands. Calculations are performed using the gradient-corrected PBE functional²⁰ as implemented in the DMol3 package.²¹ A numerical atomic basis set of double- ζ quality, augmented with additional polarization functions (DNP) is employed in this work. For Cu, the core electrons are represented with an effective relativistic semicore pseudopotential (PSPP) along with the DNP basis for valence electrons.²² The convergence criteria for structural optimizations are 1.0×10^{-7} au and 1.0×10^{-5} au/Å for energy and gradient, respectively. The calculations are carried out using a truncated cluster representation of the SiO₂ surface. The cluster model for the SiO₂ surface (using H-termination of the truncated cluster) with a stoichiometry of Si₈O₁₆H₁₆, is generated by extracting a local cluster from an extended four-layer slab of the (100)- α quartz surface. To mimic the mechanical constraints of the extended surface, the Cartesian coordinates of the lowest-layer Si atoms are fixed to the bulk SiO₂ positions during the geometry optimization and subsequent frequency calculations of the surface species described in this work. The calculated [Cu(⁸Bu-amd))₂]/SiO₂ surface structures and their corresponding simulated infrared spectra, used to support the experimental infrared band assignments reported here, are provided in the Supporting Information (Figure S1).

Figure 1 shows differential absorbance spectra of the first three cycles of Cu ALD on SiO₂ at 185 °C, where each spectrum is obtained by taking the surface of the previous half ALD cycle as a reference. Upon the first [Cu(⁸Bu-amd))₂] exposure, labeled “1st CuL” in Figure 1, there is a distinct intensity loss of the transverse and longitudinal optical modes (TO/LO) of SiO₂ at 1075/1247 cm^{−1} and the stretching/bending modes of isolated −OH moieties at 3737/1660 cm^{−1}.²³ These losses are accompanied by the appearance of a new band centered at 1010 cm^{−1}. These intensity variations are important markers for the interaction of the [Cu(⁸Bu-amd))₂] precursor with the hydroxylated SiO₂ surface. In particular, the decrease of the SiO₂ phonon modes has been

(17) Li, Z.; Barry, S. T.; Gordon, R. G. *Inorg. Chem.* **2005**, *44*, 1728–1735.

(18) Higashi, G. S.; Chabal, Y. J. In *Handbook of Silicon Wafer Cleaning Technology: Science, Technology, and Applications*; Kern, W., Ed.; William Andrew Publishing: Norwich, NY, 1994.

(19) Kwon, J.; Dai, M.; Langereis, E.; Halls, M. D.; Chabal, Y. J.; Gordon, R. G. *J. Phys. Chem. C* **2009**, *113*, 654–660.

(20) Perdew, J. P.; Burke, K.; Ernzerhof, M. *Phys. Rev. Lett.* **1996**, *77*, 3865.

(21) Delley, B. *J. Chem. Phys.* **2000**, *113*, 7756–7764.

(22) Delley, B. *Phys. Rev. B* **2002**, *66*, 155125.

(23) Conley, R. T. *Infrared Spectroscopy*; Allyn and Bacon, Inc.: Boston, **1972**.

previously correlated with chemical reactions at the SiO₂ surface,^{19,24} leading to a decrease of the overall SiO₂ phonon oscillator strength.

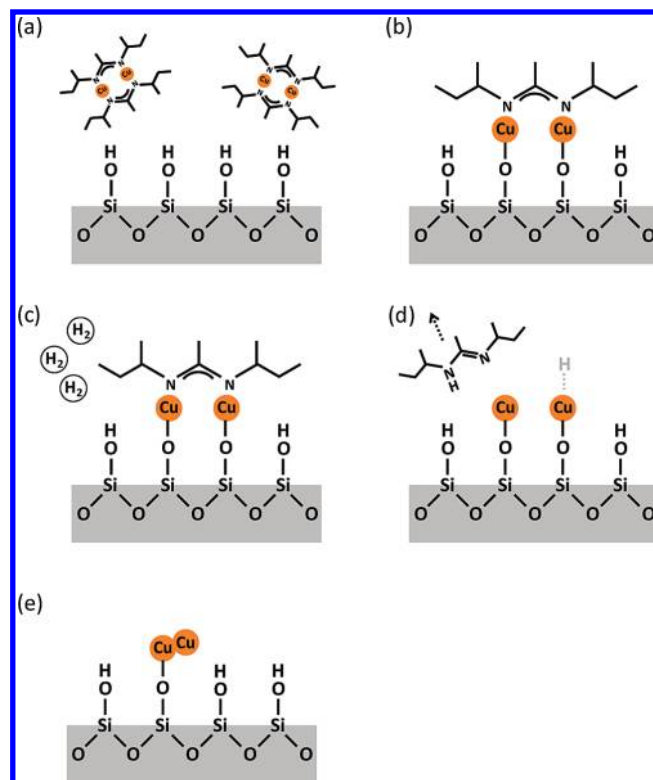
The absorption band at 1010 cm⁻¹ is in the range of the stretching vibration of Si–O bonded to a metal.^{19,24} Calculations of the vibrational modes for surface Cu₂(^sBu-amd) bonded to Si–O (originally hydroxyl sites) through the two Cu atoms confirm that the 1010 cm⁻¹ mode is associated with the formation of a Si–O–Cu–(^sBu-amd) linkage. Indeed, the computed Si–O stretching vibration for the Si–O–Cu–(^sBu-amd) species is 1018 cm⁻¹, in good agreement with the characteristic IR band at 1010 cm⁻¹. Together with the intensity loss at 3737 cm⁻¹, the increase of the Si–O–Cu stretching mode indicates that the Cu precursor reacts with the surface hydroxyl to form Si–O–Cu bonds.

The mode at 1510 cm⁻¹ is assigned to the stretching vibration of –N–C–N– of *sec*-butylacetamidate attached to Cu atoms on the surface as shown in Scheme 1, panels b and c. This assignment is based on the calculated value for the –N–C–N– stretching vibration at 1502 cm⁻¹, which is very close to the experimental observation. The behavior of the intensity of the mode at 1510 cm⁻¹ is correlated with that of CH_x stretching modes at 2800–3000 cm⁻¹, increasing after each copper precursor pulse and decreasing after each H₂ pulse. These observations are consistent with an ALD process involving ligand exchange, as schematically represented in Scheme 1, panels b–d.

After each H₂ exposure, labeled “1st, 2nd and 3rd H₂” in Figure 1, there is a partial recovery of SiO₂ phonon modes (1075/1247 cm⁻¹). The recovered intensity of the SiO₂ phonon modes indicates that the underlying SiO₂ matrix, initially covered by Si–O–Cu(^sBu-amd), is partly uncovered after an H₂ pulse. The –OH stretching vibration at 3737 cm⁻¹ exhibits a slight frequency shift (derivative line shape in differential spectra), making OH concentration changes difficult to quantify solely on the basis of OH stretching mode behavior. Examination of the –OH bending mode at 1660 cm⁻¹, on the other hand, shows a slight gain and loss in intensity after exposure to H₂ and Cu precursor, respectively. Although this band exhibits cyclic gain and loss of OH bonds, the weakness of this cyclic change suggests that the Cu precursor might also react with the oxide surface even without surface OH groups.

Molecular hydrogen is expected to form Cu–H bonds as an temporary intermediate species after removing surface ligands (Scheme 1d) because the ligand is itself hydrogenated.¹⁹ This situation is different from molecular H₂ dissociation on clean single crystal copper surfaces, which is unfavorable.²⁵ To see whether hydrogen atoms remain attached to the Cu atoms in step d of Scheme 1, a search for Cu–H or Cu–D was performed by using H₂ and D₂ gases. For reasonable concentrations of Cu–H, absorption bands within the 1700–2300 cm⁻¹ region (Cu–H stretching mode) should be detectable, although weak. It is known that hydrogen atoms in copper hydrides can be bonded to several Cu atoms, forming hydrogen bridges, thus weakening the intensity of the mode.²⁶ No Cu–H (or Cu–D) absorption bands could be identified in the relevant spectral range when spectra resulting from H₂ and D₂ treatments were compared. This is a consequence of either a low cross-section (broadening, low coverage) or a short lifetime of Cu–H bonds on the time scale of the measurements. In the latter case, any hydrogen atom temporarily attached to Cu as in Scheme 1, step d, recombines and

Scheme 1. Schematic of Reactions of [Cu(^sBu-amd)]₂ (a,b) and H₂ (c,d) on the SiO₂ surface^a



^aA free amidine in panel d represents a gas-phase byproduct after ligand removal by H₂. Panel d shows a possible intermediate Cu–H bond, which is not observed experimentally (possibly due to its very short lifetime at 185 °C). Panel e shows agglomeration of Cu atoms in a schematic way.

desorbs by the time the spectra are collected, and the free copper atoms agglomerate as in step e.

The temperature dependence of the surface reaction during the first ALD cycle is presented as differential spectra in Figure 2. At 100 °C, the Cu precursor reaction with the surface is moderate. But the featureless differential spectrum after H₂ indicates that H₂ does not reduce the surface-bound Cu precursor at 100 °C. At 140 °C, H₂ does reduce the Cu precursor as evidenced by the loss of –N–C–N– mode at 1510 cm⁻¹ and CH_x stretching modes around 2957 cm⁻¹, but the recovery of the intensity of SiO₂ TO/LO modes after the H₂ dosing is very weak. Above 140 °C, the gain of SiO₂ phonon modes is now clearly observed after H₂ pulses. Figure 2 also shows the evolution of another mode at 1605 cm⁻¹ together with the 1510 cm⁻¹ mode at low (100 °C) and higher temperature (≥220 °C), which will be discussed later.

The absorbance spectra of subsequent cycles up to 20 cycles (all referenced to the initial SiO₂ surface) are presented in Figure 3. Two different incidence angles, one close to the Brewster angle (~74°) (Figure 3a) and the other close to normal incidence (Figure 3b), are used to distinguish the modes that are parallel and perpendicular to the surface. The strong peaks at 1010 cm⁻¹ and 1112 cm⁻¹ with a shoulder at 1180 cm⁻¹ are unpolarized (i.e., not specifically related to LO modes). The intensity of the mode associated with Si–O–Cu bonds at 1010 cm⁻¹ saturates around 20 ALD cycles, as shown in the inset of Figure 3a. The intensities of the modes at 1112 cm⁻¹ and 1180 cm⁻¹, on the other hand, continue to increase linearly even after 20 ALD cycles, as shown in the inset of Figure 3b.

(24) Kwon, J.; Dai, M.; Halls, M. D.; Chabal, Y. J. *Chem. Mater.* **2008**, *20*, 3248–3250.

(25) Michelsen, H. A.; Auerbach, D. J. *J. Chem. Phys.* **1991**, *94*, 7502–7520.

(26) James, C.; Warf, W. F. *Helv. Chim. Acta* **1950**, *33*, 613–639.

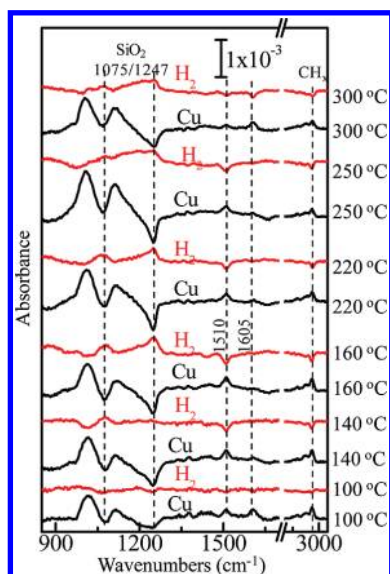


Figure 2. Differential absorbance spectra of the first cycle of Cu ALD on oxide as a function of temperatures from 100 °C up to 300 °C. The spectra of the initial half cycle after Cu precursor pulse (black) are referenced to oxide spectra and those of the one full cycle after H₂ pulse (red) to those of half cycles. The incidence angle of infrared beam is 74° (~Brewster angle).

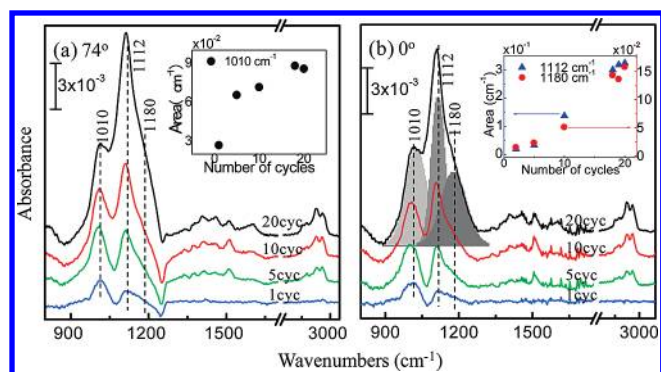


Figure 3. Absorbance spectra during Cu ALD on SiO₂/Si up to 20 cycles referenced to the initial oxide surface at 74° (a) and 0° (b) incidence angle. The inset of panel a is integrated area under the mode at 1010 cm⁻¹, and that of panel b is under 1112 (blue) and 1180 cm⁻¹ (red). An example of deconvolution into three peaks at 1010, 1112, and 1180 cm⁻¹ is shown for the 20-cycle spectrum in gray color in panel b.

The details of the ALD process (i.e., evolution of the vibrational modes) are presented in Figure 4 as differential spectra measured after the 20th Cu-precursor/H₂ pulse. The ligand exchange behavior, characteristic of an ALD process, is evident. The intensities of the CH_x stretching vibration around 3000 cm⁻¹, -N-C-N- stretching at 1510 cm⁻¹, CH_x deformation at 1367/1335 cm⁻¹ and at 983 cm⁻¹ increase after Cu precursor exposure and decrease after H₂ exposure. There is also an cyclic behavior of the SiO₂ phonon mode intensity, characterized by a loss of intensity upon Cu precursor exposure and a partial recovery of this intensity during the H₂ pulse, particularly evident for SiO₂ LO mode at 1247 cm⁻¹ in “20 cycle_Cu” spectrum measured at the Brewster angle (red) in Figure 4.

The absorption band in the 1100 to 1200 cm⁻¹ spectral range contains more than one component, as observed during the initial growth. The mode at 1107 cm⁻¹ has a shoulder at the higher frequency at ~1180 cm⁻¹ after Cu precursor exposure, as shown

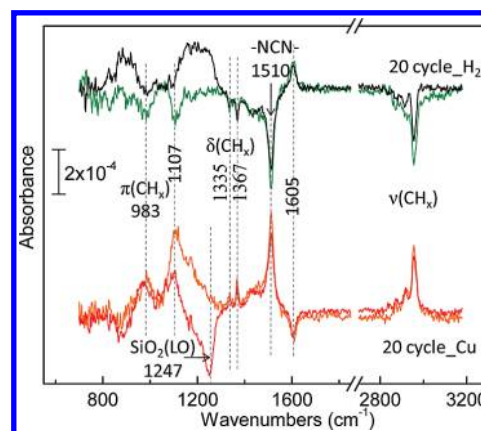


Figure 4. Differential absorbance spectra of the 20th cycle after Cu-precursor and H₂ pulses referenced to each previous treatment at 74° (red and black) and 0° (yellow and green) incidence angles.

in the spectrum labeled “20 cycle_Cu” taken at normal incidence (yellow) in Figure 4. Only a portion of the 1107 cm⁻¹ component of this band, assigned to C–C skeletal mode of *sec*-butylacetamidinate bound to Cu (DFT calc: 1105 cm⁻¹), is removed after H₂ exposure. It is easy to see in the normal-incidence spectra (yellow and green) that a significant portion of the 1107 cm⁻¹ mode and all the intensity of the shoulder at 1180 cm⁻¹ remain after the H₂ exposure. A new broadband appears in the range 1150 to 1250 cm⁻¹ after H₂ exposure (black spectrum), with LO characteristics (i.e., observed only with 74° incidence). This LO-like mode centered around 1200 cm⁻¹ can be assigned to a perturbation of the SiO₂ LO mode by Cu atoms. Indeed, it is observed that, when metallic atoms are incorporated in the SiO₂ matrix, the LO mode is shifted to a lower wavenumber, probably due to disorder caused by metallic atoms in Si–O–Si bondings. Calculation of the Γ -point phonons for bulk SiO₂-quartz shows that Cu incorporation gives rise to lattice modes at ca. 1200 cm⁻¹. (Calculated Γ -point spectra are provided in Figure S2 of the Supporting Information.)

In the normal incidence spectrum, the mode at 1107 cm⁻¹ with the shoulder at 1180 cm⁻¹ remaining after H₂ reduction (i.e., no variation is seen in the green spectrum) can be assigned to Si–O–C–R bonds,^{27,28} as discussed below. If this is the case, then this mechanism would explain an initial bonding configuration of ligands or partial ligands on the oxide and account for possible C (or N-) contamination on the SiO₂ (i.e., at the interface). These observations are consistent with the presence of vibrational modes of hydrocarbon and NC-related species in the range of 2800–3000 cm⁻¹ and 1300–1700 cm⁻¹ in Figure 3.

In Figure 4, there is a mode at 1605 cm⁻¹ with intensity variations opposite to the rest of the ligand-related modes; i.e., loss of intensity after [Cu(⁸Bu-amd)]₂ pulse and gain after H₂ pulse. This mode at 1605 cm⁻¹ can be unambiguously attributed to a monodentate configuration of the hydrogenated ligand, suggesting that a rearrangement of the ligand from a bridging to a monodentate structure takes place upon H₂ exposure. This observation provides an indirect evidence of a Cu(II) surface intermediate. Calculations are carried out for the hydrogenated amidinate ligand bound to a surface Cu–O–Si species in a monodentate configuration. They show that there is a mode involving the coupling of N–C–N– stretching and N–H bending vibrations with a mode at 1601 cm⁻¹, in excellent agreement

(27) Michalak, D. J.; Rivillon, S.; Chabal, Y. J.; Esteve, A.; Lewis, N. S. *J. Phys. Chem. B* **2006**, *110*, 20426–20434.

(28) Michalak, D. J.; Amy, S. R.; Estève, A.; Chabal, Y. J. *J. Phys. Chem. C* **2008**, *112*, 11907–11919.

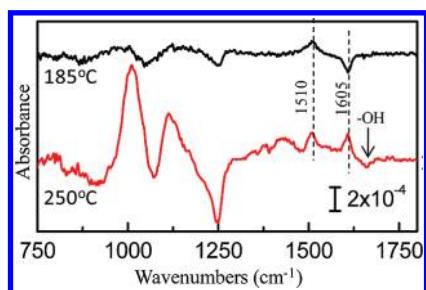


Figure 5. Differential absorbance spectra after the first Cu precursor pulse at 250 °C referenced to the initial SiO₂ (red). The surface is then exposed to the Cu precursor again at 185 °C (black) and referenced to that of the previous spectrum of 250 °C.

Table 1. Calculated PBE/DNP Wavenumbers and Mode Assignments Corresponding to the Main Observed Infrared Absorption Modes

observed IR (cm ⁻¹)	calculated (cm ⁻¹)	assignment
983	973	—CH _x deformation of ^s Bu-amd ligand
1010	1018	Si—O stretching of Si—O—Cu—(^s Bu-amd)
1107	1105	C—C skeletal mode of Cu—(^s Bu-amd)
1180	1184	C—N skeletal mode + CH _x deform of ^s Bu-amd ligand
1200	1193	Cu incorporated SiO ₂ phonons
1335/1367	1338/1383	—CH _x deformation of ^s Bu-amd ligand
1510	1502	N—C—N stretching of Cu—(^s Bu-amd)
1605	1601	N—C—N stretching + N—H bending (monodentate)

with the observed infrared mode at 1605 cm⁻¹. The H₂-induced monodentate ligand is then removed upon exposure to the Cu precursor as shown in Figure 4.

The temperature-activated ligand rearrangement is suggested by the spectra shown in Figure 2. In order to determine the effect of the intact Cu precursor molecules on the ligands rearranged after the very first ALD cycle, the surface was subsequently exposed to two consecutive [Cu(^sBu-amd)]₂ pulses (Figure 5). Figure 5 shows that the first [Cu(^sBu-amd)]₂ pulse generates the mode at 1605 cm⁻¹ together with 1510 cm⁻¹ at 250 °C (red). The initial temperature was intentionally set higher to enhance the mode related to the ligand rearrangement, which takes place above 220 °C. When the surface is again exposed to the second [Cu(^sBu-amd)]₂ pulse at 185 °C (black), the mode at 1605 cm⁻¹ is removed, and the intensity of the mode at 1510 cm⁻¹ increases. At the same time, the intensity of SiO₂ phonon modes further decreases, indicating that more reactive sites have been made available as a result of the removal of rearranged ligands by the second [Cu(^sBu-amd)]₂ pulse.

Table 1 summarizes the key observed infrared modes and calculated vibrational frequencies.

Ex-situ XPS measurements of the sample after 10 ALD cycles (Figure 6) show the chemical states of Cu, C, and N. All spectra are calibrated by the C1s at 284.5 eV. The low intensity of the satellite shakeup of the Cu2p at 945 and 965 eV suggests that there is little CuO after 10 ALD cycles. Instead, the deposited Cu film is most likely metallic (Cu⁰) or possibly Cu¹⁺ from Cu₂O due to air exposure. The two other peaks fitted to C1s at 285.1 and 288.1 eV can be assigned to C—N and C—O bonds of residual ligands, respectively.²⁹ The presence of (Si—)O—C— is consistent with the

vibrational mode observed at 1107 – 1180 cm⁻¹ in Figure 4. The N1s XPS spectrum in Figure 6c confirms the presence of residual ligands with C—N bonds in the thin Cu film. A contribution of oxygenated hydrocarbons due to exposure to air cannot be excluded for ex situ XPS C1s spectra. In the case of thicker (30 nm) Cu films, the C and N content is negligible according to XPS C1s and N1s spectra, as shown in the insets of Figure 6b,c.

Discussion

The results presented in the previous section provide information of the growth mechanisms of Cu ALD. The initial surface chemistry between OH-terminated SiO₂ and [Cu(^sBu-amd)]₂ takes place by displacement of one of the bridging *sec*-butylacetamidinate of [Cu(^sBu-amd)]₂, forming surface Si—O—Cu—(^sBu-amd) bonds as evidenced by the mode at 1010 cm⁻¹ in Figure 1. As schematically represented in Scheme 1c–e, the subsequent H₂ pulse breaks the Cu—N bonds of the surface precursor, reducing it to Cu atoms, which then migrate and self-agglomerate to form copper particles.^{12,30,31}

The formation of Cu—H is expected for the direct ALD growth on the Cu clusters, providing an alternative reaction channel to the ALD growth on the bare SiO₂ regions. Unfortunately, experimental confirmation was not possible due to the low IR cross section of Cu—H and the short lifetime of Cu—H bonds.

As the Cu atoms agglomerate, the chemical bonds between Cu and the underlying SiO₂ matrix are broken, thus causing the loss of the intensity of the mode at 1010 cm⁻¹ of Si—O—Cu and partially restoring the SiO₂ TO/LO modes at 1075/1247 cm⁻¹. The recovery of the SiO₂ TO/LO with H₂ pulse is not observed unless the surface was previously exposed to the Cu precursor, confirming that the gain of the SiO₂ phonon mode intensity is not due to additional SiO₂ growth but due to exposure of the underlying SiO₂ surface caused by Cu agglomeration. Cu agglomeration observed in the repetitive formation and breakage of Si—O—Cu bonds and gain and loss of SiO₂ phonon intensity continues even at the 20th ALD cycle, although the magnitude of the intensity variations becomes weaker. It is not likely that the surface is completely saturated after 20 ALD cycles because the percolation thickness of Cu on glass is very high.¹²

Copper agglomeration and diffusion are activated processes.^{14,32} At 140 °C, H₂ removes the surface Cu *sec*-butylacetamidinate as evidenced by the loss of —N—C—N— mode at 1510 cm⁻¹ and CH_x stretching modes around 2957 cm⁻¹ as shown in Figure 2. But the recovery of the intensity of SiO₂ TO/LO modes after the H₂ dosing is very weak. Starting with the second cycle at 140 °C and the 10th cycle at 125 °C, however, Cu agglomeration is observed again, as evidenced by the partial recovery of SiO₂ TO/LO modes (not shown), which indicates that the agglomeration takes place only when Cu reaches a critical thickness on the oxide surface.^{33,34}

As illustrated by Scheme 2, the Cu precursor reacts with a hydroxyl group on the SiO₂ surface to liberate one free amidine (a hydrogenated *sec*-butylacetamidinate ligand) into the gas phase, leaving one ligand bonded to the Cu in a bridging structure characterized by the —N—C—N— mode at 1510 cm⁻¹.

(30) Yang, C.-Y.; Jeng, J. S.; Chen, J. S. *Thin Solid Films* **2002**, 420–421, 398–402.

(31) Ching-Yu, Y.; Chen, J. S. *J. Electrochem. Soc.* **2003**, 150, G826–G830.

(32) Zhou, J. B.; Gustafsson, T.; Garfunkel, E. *Surf. Sci.* **1997**, 372, 21–27.

(33) Offerman, S. E.; van Dijk, N. H.; Sietsma, J.; Grigull, S.; Lauridsen, E. M.; Margulies, L.; Poulsen, H. F.; Rekaveldt, M. T.; van der Zwaag, S. *Science* **2002**, 298, 1003–1005.

(34) Tu, K.-N.; Mayer, J. W.; Feldman, L. C. *Electronic Thin Film Science: For Electrical Engineering and Materials Scientist*; Prentice Hall: Upper Saddle River, NJ, 1996.

(29) Moulder, J. F.; Stickle, W. F.; Sobol, P. E.; Bomben, K. *Handbook of X-ray Photoelectron Spectroscopy*; Chastain, J., Ed.; Perkin-Elmer Corporation (Physical Electronics Division): Eden Prairie, MN, 1992.

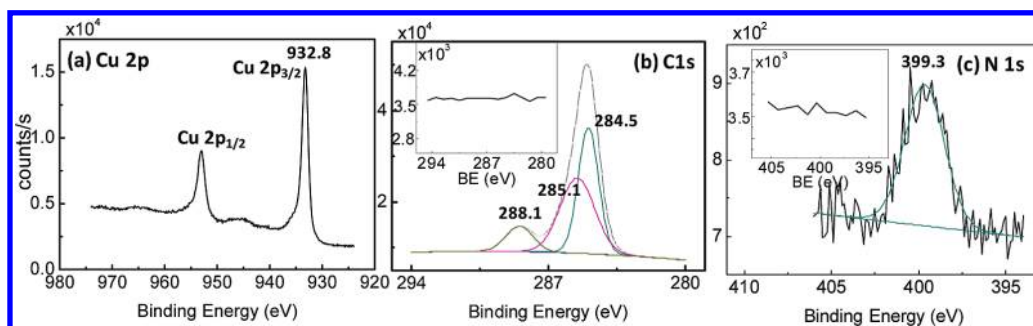
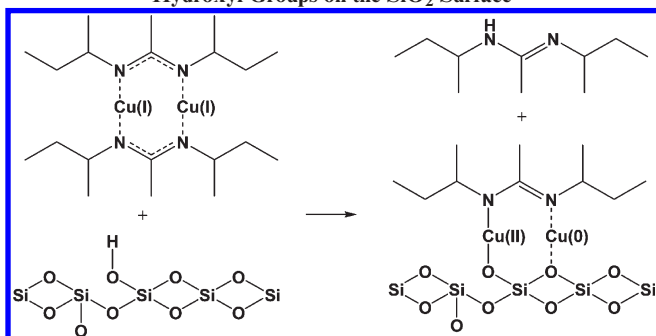
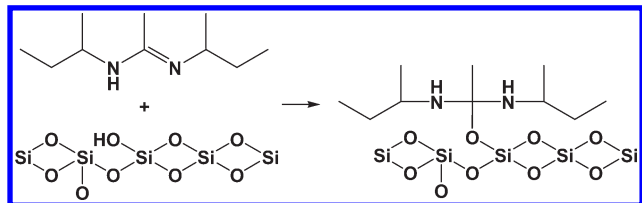


Figure 6. XPS of Cu 2p (a), C 1s (b), and N 1s (c) of 10-cycle Cu film. The insets of (b) and (c) are C 1s and N 1s of thicker (30 nm) Cu films, respectively.

Scheme 2. Possible Chemisorption Reaction of $[\text{Cu}^{\text{tBu-amd}}]_2$ with Hydroxyl Groups on the SiO_2 Surface



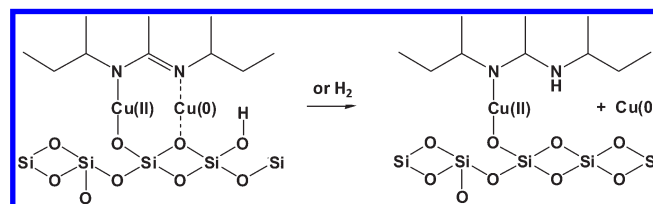
Scheme 3. Possible Chemisorption Reaction of Amidine with Hydroxyl Groups on a SiO_2 Surface



Some of the free amidine produced after chemisorption of $[\text{Cu}^{\text{tBu-amd}}]_2$ may be reattached to the SiO_2 surface, forming Si–O–C bonds. A possible mechanism for this process is shown in Scheme 3.

The insertion of a surface silanol group into the amidine double bond provides a means to attach the hydrogenated ligand to the surface, thus forming a Si–O–C bond. The IR absorption corresponding to Si–O–C bonds at 1107 and 1180 cm^{-1} in Figure 4 shows that, once formed on the SiO_2 surface, these bonds are not easily attacked by H_2 . The integrated area under these modes in the inset of Figure 3b also shows that the Si–O–C formation continues after 20 ALD cycles on this partially covered oxide surface. It is less likely that an intact *sec*-butylacetamidinate is directly bonded to SiO_2 by forming Si–O–N bonds because the XPS spectrum of the N1s core level (Figure 6c) indicates that N atoms are mainly bonded to C, with negligible contribution from N–O. The presence of N–C can be attributed to the surface bonded amidine (Scheme 3) and incomplete ligand removal by H_2 (Scheme 1). The overall measured N concentration derived from XPS peak intensity is low (less than $\sim 4\%$), whereas the mechanism in Scheme 2 results in 20% N atomic ratio relative to that of C. In other words, the relatively high C concentration detected in the ex situ XPS measurements is due to environmental contamination during the transfer from the reactor to the XPS chamber.

Scheme 4. Hydrogenation of an Amidinate Ligand on a Cu/SiO_2 Surface with Rearrangement from a Bidentate to a Monodentate Binding of a Saturated Amine



According to independent experiments, the carbon and nitrogen content of thicker (30 nm) Cu films measured by XPS is negligible (insets of Figure 6b,c), which indicates that incorporation of C and N impurities, if any, mainly takes place by insertion of free amidine groups to the exposed SiO_2 substrate during the initial film growth before the surface is covered by Cu.

In addition to agglomeration, Cu atoms are also incorporated into the first few layers of the SiO_2 matrix at a deposition temperature of 185 $^{\circ}\text{C}$. The presence of metallic Cu atoms in the SiO_2 layer causes disorder in the Si–O bonds, which results in the LO mode shift to a lower frequency as observed by the broad mode after H_2 reduction in the region of 1150–1250 cm^{-1} in Figure 4 (black). Cu incorporation into the SiO_2 substrate continues even after 20 ALD cycles. Cu agglomeration is also observed on other oxides such as ALD grown Al_2O_3 , but is suppressed on thermally grown Si_3N_4 , indicating the stronger bonding between Cu atoms and nitride surfaces compared to oxide surfaces (data not shown).

During the first few ALD cycles, the presence of hydrogen in the surface hydroxyl groups can cause hydrogenation of the surface ligand, inducing a rearrangement from a bridging to a monodentate structure (Figure 2 and 5). The secondary amine in the monodentate ligand has the vibrational mode at 1605 cm^{-1} (cal. 1601 cm^{-1}). The ligand rearrangement is accompanied by release of a copper atom, as suggested in Scheme 4. These saturated monodentate ligands can be displaced by more basic amidine groups during the next dose of H_2 (Figure 2) or $[\text{Cu}^{\text{tBu-amd}}]_2$ (Figure 5). Note that amidine groups are released after both a $[\text{Cu}^{\text{tBu-amd}}]_2$ pulse (Scheme 2) and a H_2 pulse (Scheme 1). This hydrogenation reaction is temperature activated, occurring above 220 $^{\circ}\text{C}$ as shown in Figure 2. A mode near 1605 cm^{-1} also appears at lower temperatures below 140 $^{\circ}\text{C}$, indicating that a second pathway to another secondary amine may exist, such as, for example, the insertion suggested in Scheme 3.

After almost all surface hydroxyl groups are reacted and more Cu atoms are formed on the surface, the activation temperature of the ligand rearrangement is lowered to at least 185 $^{\circ}\text{C}$, and hydrogenation of the ligand is now aided by H_2 pulses as shown in Figure 4. Copper metal has some activity as a hydrogenation

catalyst, causing the presence of nearby copper clusters to promote the hydrogenation step. These monodentate ligands are displaced by free amidine released during the consecutive Cu precursor pulses.

Conclusions

The initial surface chemistry and growth mechanisms of ALD of copper on the SiO₂ surface with copper(I) di-*sec*-butylacetamidinate ([Cu(^sBu-amd)]₂) and H₂ have been investigated and discussed. The initial surface reaction is through displacement of one of the *sec*-butylacetamidinate ligands by a surface –OH group, thus forming Si–O–Cu bonds with one ligand still bound to the surface. The subsequent H₂ pulse removes surface ligands, leaving Cu atoms free to agglomerate on and be incorporated into the SiO₂ substrate. The thermally activated ligand rearrangement from a bridging to a monodentate structure occurs above 220 °C through hydrogenation of the ligand by surface hydroxyl groups after exposure to [Cu(^sBu-amd)]₂ pulses. As the Cu particles grow on the surface with further ALD cycles, the activation temperature is lowered to 185 °C and hydrogenation of the ligand takes place after H₂ pulses. The surface ligand rearranged into a monodentate structure can be removed by more basic amidine groups released during subsequent Cu precursor or H₂ pulses. The

carbon content at the Cu/SiO₂ interface arises mostly from Si–O–C bonds between the SiO₂ surface and dissociated ligands that remain attached even after H₂ pulses.

We have shown that monoelemental Cu growth by ALD involves complicated surface chemistry. Understanding growth mechanisms, effects of temperature on Cu agglomeration/diffusion and pathways of possible impurity incorporation is important for future applications such as Cu metallization in microelectronics, as well as further development of suitable metal precursors for a variety of applications.

Acknowledgment. This work was supported by the National Science Foundation (CHE-0415652). The copper precursor was provided by the Dow Chemical Company. Youbo Lin and Yeung Au prepared the thicker copper film and took its XPS spectrum. Harish Bhandari loaded the bubblers with the Cu precursor.

Supporting Information Available: Calculated infrared spectra for the key surface species implicated in this work to support the experimental infrared band assignments, and details about the spectral deconvolution procedure. This information is available free of charge via the Internet at <http://pubs.acs.org/>.